Technical Note

Landslides
DOI 10.1007/s10346-024-02292-y
Received: 22 May 2023
Accepted: 20 May 2024The
Author(s) 2024

Guadalupe Bru · Pablo Ezquerro · Jose M. Azañón · Rosa M. Mateos · Meaza Tsige · Marta Béjar-Pizarro · Carolina Guardiola-Albert

Deceleration captured by InSAR after local stabilization works in a slow-moving landslide: the case of Arcos de la Frontera (SW Spain)

Abstract Interferometric synthetic aperture radar (InSAR) is a remote sensing tool used for monitoring urban areas affected by geological hazards. Here we analysed the effectiveness of stabilization works on a slow-moving landslide in Arcos de La Frontera (Cádiz, Spain) using a persistent scatterer interferometric approach. The works consisted on jet grouting of cement-based injections and were applied locally to stabilize the most damaged neighbourhood. We processed a large stack of Sentinel-1 SAR satellite acquisitions covering the period January, 2016, to March, 2023, and obtained surface velocity and displacement trends measured along the line of sight (LOS) of the satellite on both ascending and descending orbits. The results show a clear deceleration of the landslide head after mid-2018, suggesting the local stabilization works were effective after that time. Prior to mid-2018, the maximum LOS velocity of the landslide head was 2.2 cm/year in ascending orbit and 1.3 cm/year in the descending orbit, decreasing to 0.43 cm/year and 0.23 cm/year, respectively. The InSAR results were compared to in-situ monitoring data and revealed that the extent of the stabilization has influenced a much larger area beyond the zone of the local interventions. Overall, InSAR has proved a powerful and versatile tool to be implemented in operational geotechnical monitoring.

Keywords InSAR · Geotechnical monitoring · Urban landslide · Stabilization works

Introduction

Landslides are a globally widespread natural hazard that occurs under various environments and conditions, with the potential to lead to fatalities and economic losses. They can develop not only in mountainous regions but also in moderate relief areas with unfavourable geotechnical conditions (weak rock and soil). A landslide, broadly defined, describes the movement of a mass of geological material, which can originate from diverse sources and possess various geomechanical properties, sliding down a slope (Hungr et al. 2014). This includes a large variety of phenomena, with their own peculiar features and mechanical behaviour. Within the wide spectrum of landslide types, slow moving slides are characterized by motion rates that span several centimetres per year and can persist for years to decades. Numerous natural, human-induced, or a combination of triggering factors can initiate or accelerate the motion, such as high rainfall, removal of the supporting forces of the toe by river erosion, topographic reshaping of the slope, or increased loading by buildings. While slow-moving landslides rarely claim lives, they can cause significant damage to housing and infrastructure; moreover, they may serve as precursors to faster and catastrophic mass movements.

Satellite synthetic aperture radar interferometry (InSAR) is an Earth observation (EO) technique that measures the temporal evolution of ground surface deformation along the radar line-of-sight (LOS) direction, being particularly suitable to identify and/or monitor ground deformation associated with slow-moving landslides (Colesanti and Wasowski 2006; Herrera et al. 2013; Hilley et al. 2004; Solari et al. 2020; Wasowski and Bovenga 2014). For the particular case of landslides, the geometry of the slopes is a determinant factor to take into consideration, as the radar visibility for ascending or descending SAR images might be hampered. There are several InSAR methods depending on the criteria to select the punctual measuring targets (persistent or distributed scatters) and on the interferogram network formation (single of multi-reference) (Minh et al. 2020; Osmanoğlu et al. 2016). Among them, the Stanford method of persistent scatterer (StaMPS) is suited for measuring surface deformatoion in urban and non-urban environments when the man-made and natural targets remain coherent over time, even with low-amplitude phase stability (Hooper et al. 2004). Sentinel-1 (S1) SAR is a two-satellite constellation operated by the European Space Agency (ESA) at C-band, providing a medium spatial resolution of 20 × 5 m. It was launched in 2014 and initially provided freely accessible global data with a revisit time of 6 days until December, 2021. Subsequently, the revisit time extended to 12 days due to the complete failure of satellite S1B. This data provides an exceptional opportunity to monitor long-term motion of slow-moving landslides and analyse areal extent or speed changes of different periods (Cigna and Tapete 2021; Cook et al. 2023; Kalia 2023). In the current scenario of Big Data SAR archives, the European Ground Motion Service (EGMS) from the Copernicus Land Monitoring Service (CLMS) provides free access to high-resolution monitoring of ground deformations over most of Europe, based on full-resolution processing of all S1 satellite images available (Costantini et al. 2022). EGMS employs advanced persistent scatterer (PS) and distributed scatterer (DS) InSAR processing techniques. At the time of writing, the EGMS products cover the period February, 2015, to December, 2022, and updates are planned annually thereafter (CLMS 2023).

Landslide monitoring means the comparison of landslide conditions (like areal extent, speed of movement, topography, or soil humidity) from different periods in order to assess landslide activity (Mantovani et al. 1996) and to interpret its mechanical behaviour. Designing optimal engineering solutions to minimize the intensity of landslide hazard phenomena or reduce the

vulnerability of exposed urban elements at risk should follow a thorough understanding of the process and the characterization and quantification of geo-mechanical properties. The scope of geotechnical instrumentation during the construction or operation phase of a stabilization or remedial project is to monitor field performance and to evaluate and update the design judgements if necessary (Dunnicliff 1993). The implementation of InSAR techniques in the operational geotechnical monitoring of landslides provides valuable and complementary information to in situ instrumentation data (Bru et al. 2018; Ciampalini et al. 2021; Cigna et al. 2017; Guilhot et al. 2021) and allows the identification of urban landslides based on LOS velocity distribution (e.g. Guerriero et al. 2019). InSAR has the advantage of being cost-effective, as there is no need to involve staff in field campaigns, direct data collection, and maintenance of continuous recording systems, plus there are numerous open-source InSAR processing packages (Hooper 2008; Sandwell et al. 2011; Yunjun et al. 2019) and the option to access free satellite data. Moreover, it offers spatially extensive information compared to in situ methods and provides long observation periods with fixed-time acquisitions, unlike other remote techniques. The effectiveness of engineering stabilization works on unstable slopes has been assessed a posteriori using InSAR displacement rates from different satellites (Czikhardt et al. 2017; Del Soldato et al. 2018; Di Maio et al. 2018; Liu et al. 2020) and during and after the interventions (Confuorto et al. 2019).

Arcos de la Frontera is a National historic-artistic monumental town located in the province of Cádiz (Andalusia, Spain) that went through a vast urban expansion in the first decade of this century. New housing blocks were constructed on a gentle slope area underlined by weathered clayey soil of the Guadalquivir Blue Marls (GBM) formation, which is extensively present in the region and typically undergoes serious geotechnical problems. GBM are high-plasticity clays that behave as a stiff soil with very low strength parameters when they are weathered (Escolano Sánchez et al. 2019; Tsige and Corral 2013). Numerous geotechnical failures such as landslide subsidence, collapse, soil creep, and expansiveness in the Guadalquivir basin are related to this formation (Alonso and Gens 2006; Oteo 2000; Tsige et al. 1995; Uriel and Fornes 1994; Uriel and Oteo 1976). Arcos de la Frontera landslide activity has caused damages of various degrees to infrastructures, urban assets, and buildings in the New Town area since the 1970s. The most affected site is La Verbena neighbourhood, comprised of five buildings that exhibited slope motion shortly after their construction in 2007. In October, 2009, 22 families were evacuated due to severe structural damage of one of the buildings, which was definitely declared derelict in March, 2010, after an intense precipitation period. Remediation measures to locally stabilize the slope motion in La Verbena were implemented intermittently between 2011 and 2021 with a cost of 4.1 million €. Previous research studies on this landslide have focused on the geological and mechanical characterization of the process, based on InSAR measurements along with a detailed geological interpretation and urban damage distribution (Bru et al. 2017). In another study, a methodology was developed to map vulnerable buildings in urban areas affected by active landslides using this site as a test scenario (Béjar-Pizarro et al. 2017). The landslide motion rates measured in these works using InSAR techniques reached up to 3 cm/year in the satellite line of sight (LOS) during the periods April, 2011, to February, 2012, and February, 2015, to July, 2016.

In the present study, we comprehensively review the technical documentation related to urban damages caused by slope instability in Arcos de la Frontera New Town area since 1970, including the field investigations and the local stabilization works commissioned by the local authorities. We carried out on-site field assessments to document urban damages and geomorphological features. We conducted an analysis of landslide activity in the Arcos de la Frontera New Town area spanning a 7-year period, from January, 2016, to March, 2023. The InSAR analysis is based on Sentinel-1 SAR data acquired in both ascending and descending orbits. The displacement time series (TS) reveal a change in the trend after mid-2018, suggesting a deceleration in sliding. We further analyse the changes in landslide activity and establish correlations with the local stabilization works undertaken in the La Verbena area. Additionally, we compare our InSAR results with those provided by the European Ground Motion Service (EGMS).

Study area

Geology and geomorphology

Arcos de la Frontera (Andalusia, Spain) is located in a small post-orogenic intramountain basin that is part of the geological domain of the Guadalquivir Basin (Sanz de Galdeano and Vera 1992). The site's geomorphology is characterized by the erosion of different Miocene materials by the Guadalete River, which flows at the base of the town (Fig. 1). The old town is perched on a nearly vertical 100-m cliff, where calcarenites are exposed. In the gentler slopes to the west, where a portion of the new town is settled, high-plasticity silty clays from the GBM formation are prevalent (VORSEVI 2009). Moving towards the lower part of the slope, the GBM exhibits a higher clay content, contributing to a smoother landscape with slopes measuring less than 15°. Alluvial plain materials are deposited in the inner bank of the Guadalete River. Soil samples collected at the head of the landslide and at the Tablellina water channel during various field investigations, as documented in technical reports (García 1970; VORSEVI 2009, 2010), reveal a distinct stratification in the GBM. The upper layer consists of weathered high-plasticity GBM, identified as brown silty clays with variable thickness, transitioning to an increased clay content. Immediately below, at depths of around 15–20 m, unweathered high-plasticity GBM are found, characterized by a green-grey colour. Dynamic probing super heavy (DPSH) and standard penetration tests (SPT) conducted in these investigations classified the consistency of weathered GBM as soft to medium in the shallower part and stiff to hard below. Meanwhile, the unweathered GBM were classified as hard.

The investigated landslide develops on the western slope where the GBM formation is present (Fig. 1). According to the classification by Hungr et al. (2014), it falls into the category of a planar slide earthflow. The displaced material initially undergoes planar slide movements before transitioning into a flowing state. The lower sections of the slope are the first to fail, primarily influenced by river erosion. Consequently, new slides form through a series of progressive retrogressive failures upslope (Béjar-Pizarro et al. 2017). The location of the main scarp is determined by the contact between the calcarenites and the GBM formation. The cross section of the slope in Fig. 1b illustrates the planar surface

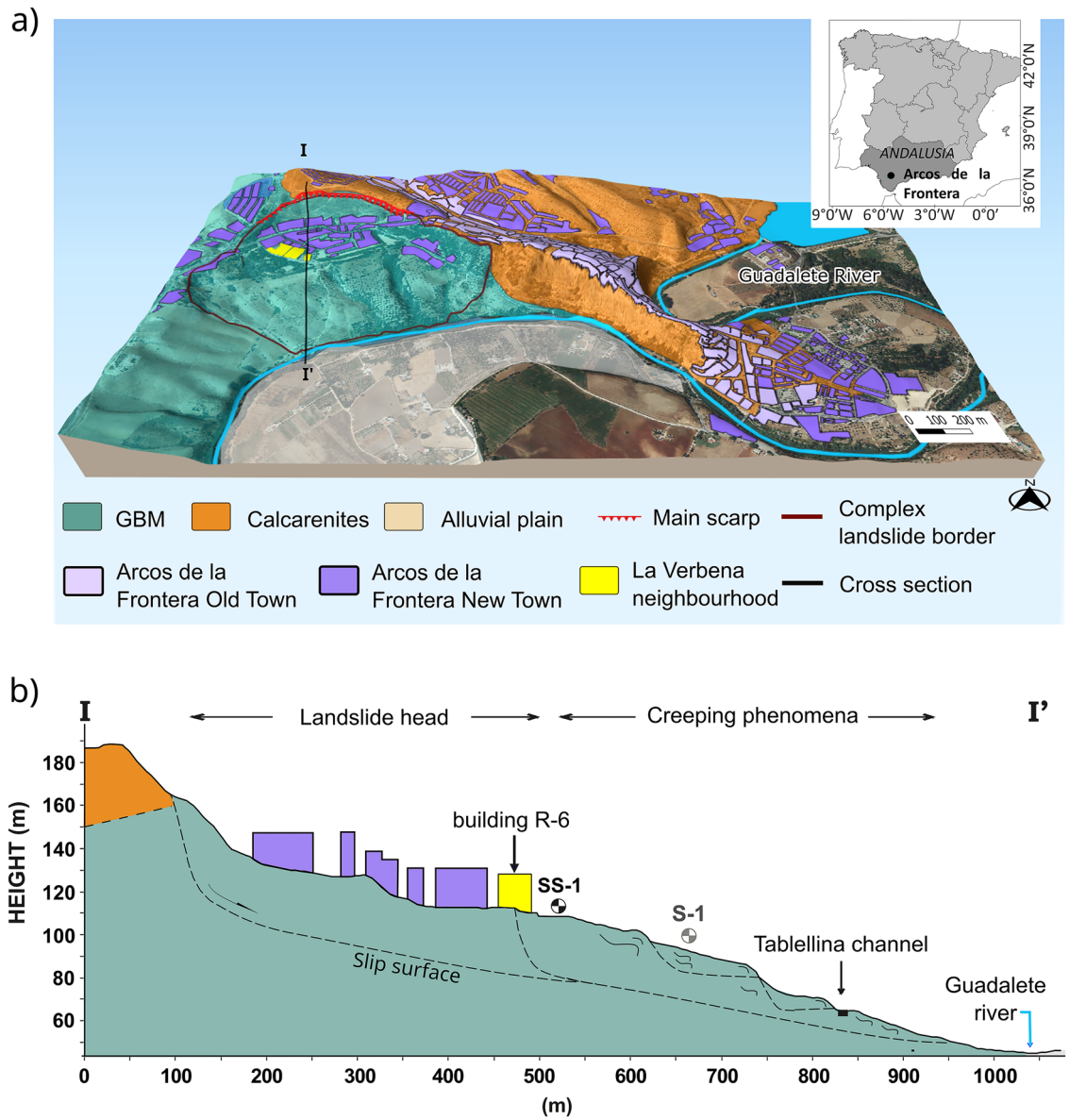

Fig. 1 **a** Location and geological map of the studied area. Buildings belonging to the Arcos de la Frontera Old Town are depicted in a different colour than those constructed after 1960 (New Town). La Verbena neighbourhood is situated at the head of the landslide, and the Guadalete River flows at the foot of the landslide. **b** Geological cross section illustrating the complex landslide. Please note that the cross section is in proximity to inclinometer S-1 but does not directly intersect with it

and shallower slips, as interpreted from field characterization along with inclinometric data (which will be further described in the "Geotechnical investigations and local stabilization works" section). The head of the landslide covers a relatively flat area of 0.17 km² and is entirely urbanized by the New Town (Figs. 1 and 2). In the medium and lower parts of the slope, soil piping and creeping phenomena are observable, along with mudflows exhibiting lobular morphologies (Fig. 3).

The principal direction of motion of the landslide in La Verbena area is identified as 330° NE, following the local maximum slope path, as observed in numerous pavement cracks (inset Fig. 2) and supported by geotechnical instrumentation data (Cobo 2021; MCH 2009). These cracks indicate the alignment of movement along this direction. Additionally, cracks observed in buildings parallel to the main scarp line suggest a N-S component of movement in the middle and eastern header area.

Urban development and damages

Arcos de la Frontera has a population of more than 30,000 inhabitants. Approximately the 80% of its buildings were constructed after the 1960s, being the most productive construction period the 1995–2009 (Figs. 2 and S1 in the Supplementary Material)

Table 1 Timeline sequence of reported damages associated with landslide motion, building construction, and local stabilization works

Year	Events
1970	A technical geological report by García (1970) identifies severe damages in the Tablellina water channel and around the old railway station caused by shallow slip processes occurring in the weathered GBM formation.
1995	The land use designation of the area where La Verbena is now settled was changed to urban land (PGOU 1995).
2000	The geotechnical investigations carried out before the construction of La Verbena buildings (TEDECO 2000) did not consider landslide hazard.
2001–2004	Construction of La Verbena buildings.
2007	First damages reported in building R-6: cracks inside the flats and opening of the dilatation joint (Dictum 2014).
2009	Preliminary survey reports and analysis of pathologies of La Verbena buildings exposing the building degradation (EDARTEC 2009; EXPERTA 2009). An expert report at the end of the year recommended declaring building R-6 derelict (MCH 2009), leading to the evacuation of 22 families. Subsequently, geotechnical works were initiated (VORSEVI 2009) to investigate possible stabilization measures.
2010	Between December, 2009, to February, 2010, more than 800 mm of accumulated rainfall aggravated the damages in building R-6, which was finally declared derelict by the Local Government Board. The geotechnical works continued (VORSEVI 2010).
2011–2014	Phases I–II (BOE 2011a, b) of local stabilization works in La Verbena, involving water drainage and jet grouting, with a total cost of €2.6 million.
2014	The families evacuated from building R-6 lose their trial against the construction company. The court determined that the damages were a result of the landslide and not due to building defects (Dictum 2014). The company argued that the slope failure was unpredictable and cited the Urban Development Plan of the city (PGOU 1995), which did not mandate a landslide hazard analysis due to the characteristics of the La Verbena site—specifically, the slope inclination being less than 15%, and the affected area or volume being less than 2500 m^2 and 5000 m^3, respectively.
2018–2021	Phase III of local stabilization works in La Verbena, involving jet grouting with a total cost exceeding €1.5 million (Moncloa 2017).
2023	Planned works for phase IV involve the renovation and restoration of urban elements, with an estimated cost of €1.5 million.

coinciding with the Spanish housing bubble. The historical old town flourished between the fifteenth to eighteenth centuries and settles on the top of a calcarenite ridge; meanwhile, the newer areas are located over gentler slopes at its sides. The geological materials underlying the western New Town area are the GBM. Evidence of mass movements in this area was documented as early as the 1970s (García 1970), with severe impacts on linear infrastructures such as the artificial water channel known as the Tablellina and the old railway station (Figs. 3 and S2 in the Supplementary Material). The latter was dismantled at the beginning of the 1980s. In 1995 a new Urban Development Plan was approved by the municipality (Table 1) and new, large areas around the town were declared as urban (PGOU 1995), including the head of the landslide. La Verbena neighbourhood is composed of five buildings constructed between 2001 and 2004, starting from those located further West at the top of the slope (inset Fig. 2). Each building is divided by two or three expanding joints and the type of foundation is reinforced concrete continuous slab. First damages appeared in building R-6 (inset Fig. 2) in 2007 in the form of cracks in partition walls, pillars and pavement, the opening of the dilatation joint, and the breakage of sewer and water systems (Dictum 2014). The rest of the buildings were gradually affected by the same structural issues (Fig. S3 in the Supplementary Material), decreasing the degree of damage from R-5 to R-2 (EDARTEC 2009; EXPERTA 2009). By October, 2009, severe structural damage of building R-6 led to the evacuation of 22 families. The reinforced concrete slab forming the foundation of the building had failed in the area near the expansion joint. This caused the settlement and tilting of the southern part of the building with respect to the other (Fig. 4), as well as the appearance of horizontal cracks in the pillars near the expansion joint and damage to the structural elements of the floor slabs. The opened joint resulted in a preferential entry of rainwater. Between December, 2009, to February, 2010, more than 800 mm of accumulated rainfall aggravated the damages and building R-6 was declared derelict by the Local Government Board. The opening of this joint in the NS direction measured in the western facade was 10 cm in 2009 (MCH 2009). In December, 2022, we measured in the same place 60 cm of opening in the NS direction, 32 cm in the WE direction, and a difference of 40 cm between buildings height vertically (Fig. 4).

Geotechnical investigations and local stabilization works

Geotechnical investigations in the La Verbena area have been ongoing since 2009, encompassing a comprehensive characterization

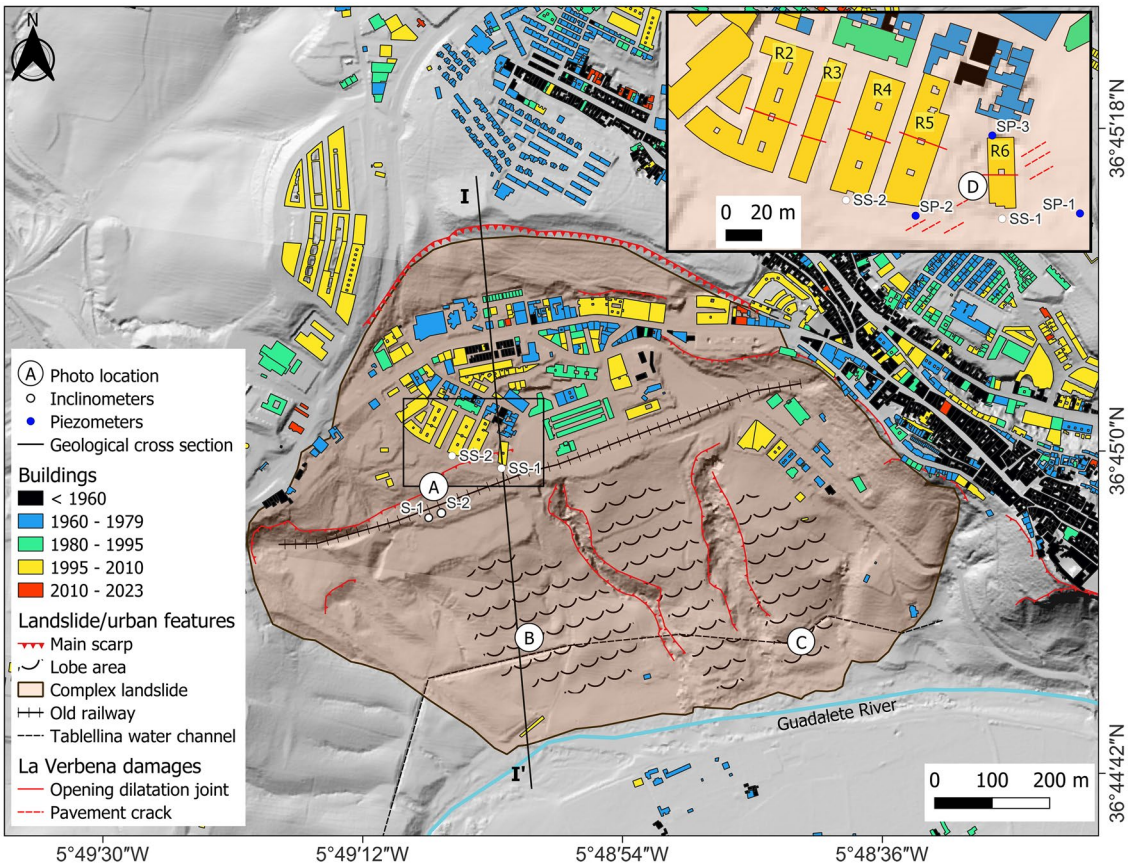

Fig. 2 Stages of building construction in the New Town of Arcos de La Frontera (see Fig. S1 in the Supplementary Material). It highlights both, the landslide and urban features. Circled letters indicate sites corresponding to the photos shown in Figs. 3 and 4. The upper right inset showcases the La Verbena neighbourhood, constructed between 2001 and 2004, with discernible damages indicated by surface cracks and openings of building dilation joints. The five buildings comprising La Verbena are labelled R2 to R6

of materials through in-situ and laboratory testing. This data is documented in various technical reports commissioned by the local authorities (Table 1). It is important to highlight that these reports, along with the plans for implementing the stabilization works, did not approach the complex landslide as a holistic problem. Instead, the focus was specifically directed towards addressing the most damaged area, which is La Verbena. On the contrary, research conducted using InSAR, geological and geomorphological mapping, and urban damage inventory (Béjar-Pizarro et al. 2017; Bru et al. 2017) revealed that the extension of the active area goes beyond La Verbena, and they delineated the boundaries of the complex landslide. The field investigations described in the technical reports involved the installation of manual recording piezometers, inclinometers, and crack gauges, as well as tachymeter surveys to monitor building movements and cross-hole seismic surveys to analyse changes in soil strength parameters after the stabilization works (which aimed to enhance the geotechnical properties of the soils). All of these aspects will be further explained in this section.

The initial geotechnical report, conducted before the construction of La Verbena, analysed soil performance to a depth of 10 m (TEDECO 2000). Despite evidence of previous damages near this site (Fig. 3) to the old railway and Tablellina channel (García 1970), the report failed to identify potential landslide hazard. Subsequently, after the complex landslide started causing damage to the buildings in 2007, more detailed investigations were conducted. In July, 2009, crack gauges were installed inside building R-6 in response to emerging damages. Monthly readings were conducted until November, 2009, revealing a progressive opening of cracks with a maximum displacement of 5 mm over the 4-month period. This observation exposed the gradual degradation of the structure (EXPERTA 2009). To investigate landslide activity, two inclinometers and three piezometers were installed in La Verbena (VORSEVI 2010). Only two manual inclinometric readings were conducted between September, 2008, and February, 2009. Inclinometer SS-1, with a length of 25 m, detected a basal slip surface at a depth of 24 m, exhibiting approximately 30 mm of cumulative landslide displacement towards the maximum slope direction. In contrast, in inclinometer SS-2, the basal slip surface was distinctly identified at a depth of 6 m, displaying cumulative displacements of less than 30 mm towards the maximum slope direction. Other inclinometers installed below the landslide head in 2003 identified a shallow slip surface at 4.5 m (S-1) and 7 m (S-2) (VORSEVI 2003). Phreatic level measurements on 11/09/08 indicated a level at 9 m depth in SS-1, while SS-2 was dry. The only available data from the piezometers, measured on 03/09/2010, showed phreatic levels

Fig. 3 Photographs of landslide impacts and features. **a**, **b** Soil piping at the old railway (site A in Fig. 2) in 1970 and 2022, respectively. **c**, **d** The Tablellina water channel in 2017 (site B in Fig. 2) in 2017 and 2022, respectively. **e** Creep processes and mudflows forming lobular morphologies (site C in Fig. 2)

at 2.5 m depth in SP-1, 4.5 m depth in SP-2, and 3.2 m depth in SP-3. These measurements were taken 2 years apart. Between December, 2009, and February, 2010, the region experienced a substantial accumulation of over 800 mm of rainfall, which could potentially explain the observed rise in the water table, reaching almost 5 m (Bru et al. 2017). High-precision tachymeter surveys were performed over La Verbena buildings between February, 2013, and June, 2021, to monitor their movement during the stabilization works. Cross-hole seismic pair surveys were also performed between 2017 and 2021 to analyse the soil properties before and after the last phase of stabilization works (Cobo 2021).

The primary purpose of the stabilization measures was to enhance the geotechnical properties of the soil beneath La Verbena neighbourhood, located at the head of the landslide, to mitigate slope movements at this specific location. The works involved draining the western part of the slope head and implementing jet grouting via boreholes to improve both bearing capacity and relative density of the ground. Phases I and II of jet grouting works were carried out

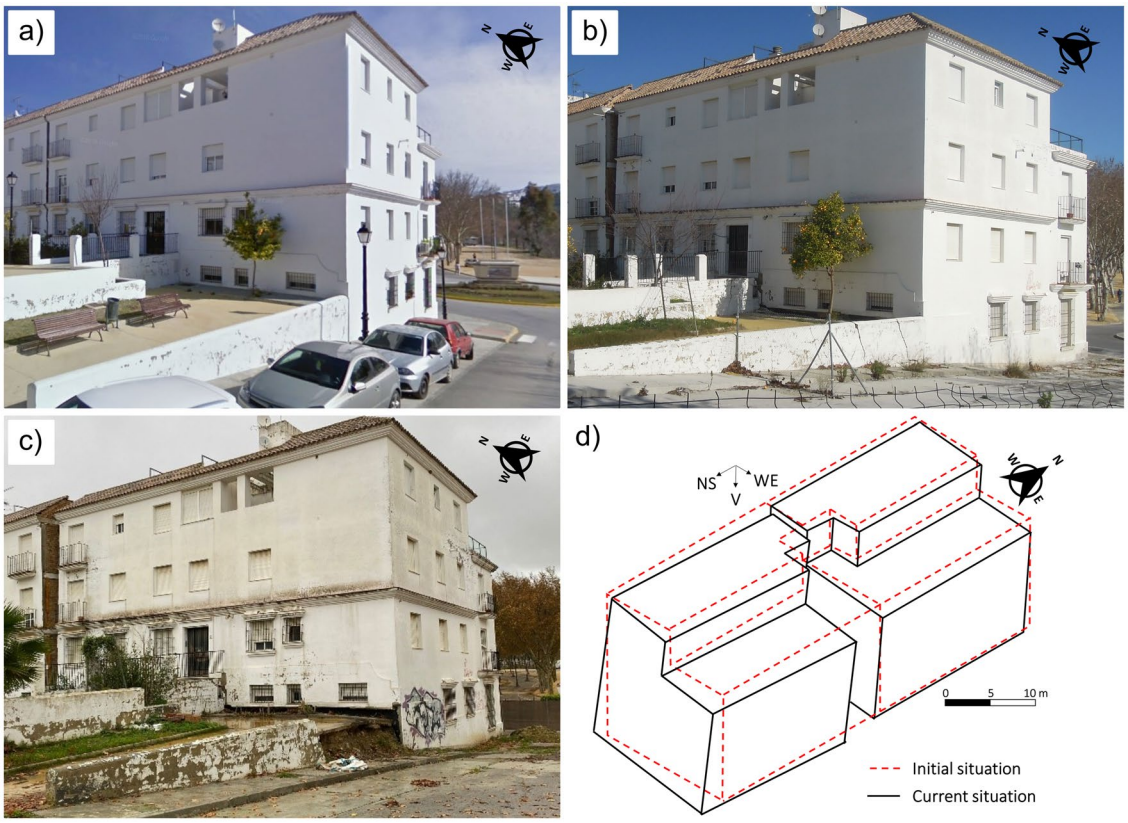

Fig. 4 Photos of building R-6 (site D in Fig. 2) showing the gradual opening of the dilatation joint through the years **a** 2009 (Google StreetView), **b** 2015, and **c** 2022. **d** Graphical representation of the displacement of the R-6 building from the time of its construction to the present day (2023)

in La Verbena neighbourhood soils between 2011 and 2014, starting in the areas labelled as TA-1 and TA-2 in Fig. 5a. Small diameter holes (76 mm) were drilled with inclinations ranging between 0° (vertical) and 45°, reaching depths up to 40 m and a drill spacing between 1 and 3.5 m (Fig. 5a and b). The jet grouting scheme is shown in Fig. 5c. A low-mobility cement mortar with high internal friction (Abrams cone between 3 and 8 cm) was pumped with a flow ranging between 10 and 90 L/min at high-pressure (between 5 and 30 bars). The pumped mortar induced lateral displacement of the soil in the vicinity of the application points, resulting in densification, hardness, and increased strength of the soil surrounding the treated area. Additionally, the reorganization of soil particles significantly reduced the percentage of voids. The vertical stress in the treated soil layer ensured that the low-mobility mortar displaced the soil horizontally without causing uplift at the surface. Tachymeter surveys in 2014 showed that the movement of the buildings in the areas TA-1 and TA-2 had not only stopped but was also partially reversed. However, the following survey in October, 2017, detected movements downslope in buildings R-2, R-3, and R-4, highlighting the urge of a third phase. Phase III started in February, 2018, and the first operation was the controlled drainage of La Verbena area with the objective of increasing shear strength and achieve primary soil consolidation. Hereafter the jet grouting works were performed in the zone TA-3. The mortar injections also facilitated soil water drainage, but disabled the draining pipes. Tachymeter surveys conducted in August, 2019, and February, 2020, indicated stabilization in area TA-3. However, adverse movements were detected in buildings within TA-1 and TA-2, leading to the spatial densification of injections along the same axes as the previous ones. The latest survey in June, 2021, revealed a reversal of movement in the zone corresponding to TA-2, showing upward movements with respect to the slope of the hillside. No movement was detected in TA-1 and TA-3 at that time.

The cross-hole seismic surveys in the TA-2 zone, conducted in 2017 and September, 2021, aimed to analyse changes in strength soil parameters before and after the jet grouting works of phase III. The results revealed a notable increase in the bulk modulus (K) by 33 to 115% and an increase in the shear modulus (G) between 60 and 250% at depths of 10 to 20 m. This enhancement in both K and G signifies improved stiffness (resistance to compression) and strength (resistance to shear forces) in the treated soils.

The significance of these parameter increases lies in reinforcing the stability of the slope. They directly contribute to the soil's resistance against sliding and shear forces, thereby enhancing load-bearing capacity. Additionally, the filling of microfissures within the GBM formation reduces permeability, minimizing water infiltration and preventing further degradation of the structural integrity of the slope. The jet grouting process induced the horizontal propagation and impregnation of the cement mortar, extending several tens of metres (more than 100 m in some cases) from the injection points at La Verbena. This suggests an improvement in geotechnical soil properties in a much wider area. However, it is important to note that the

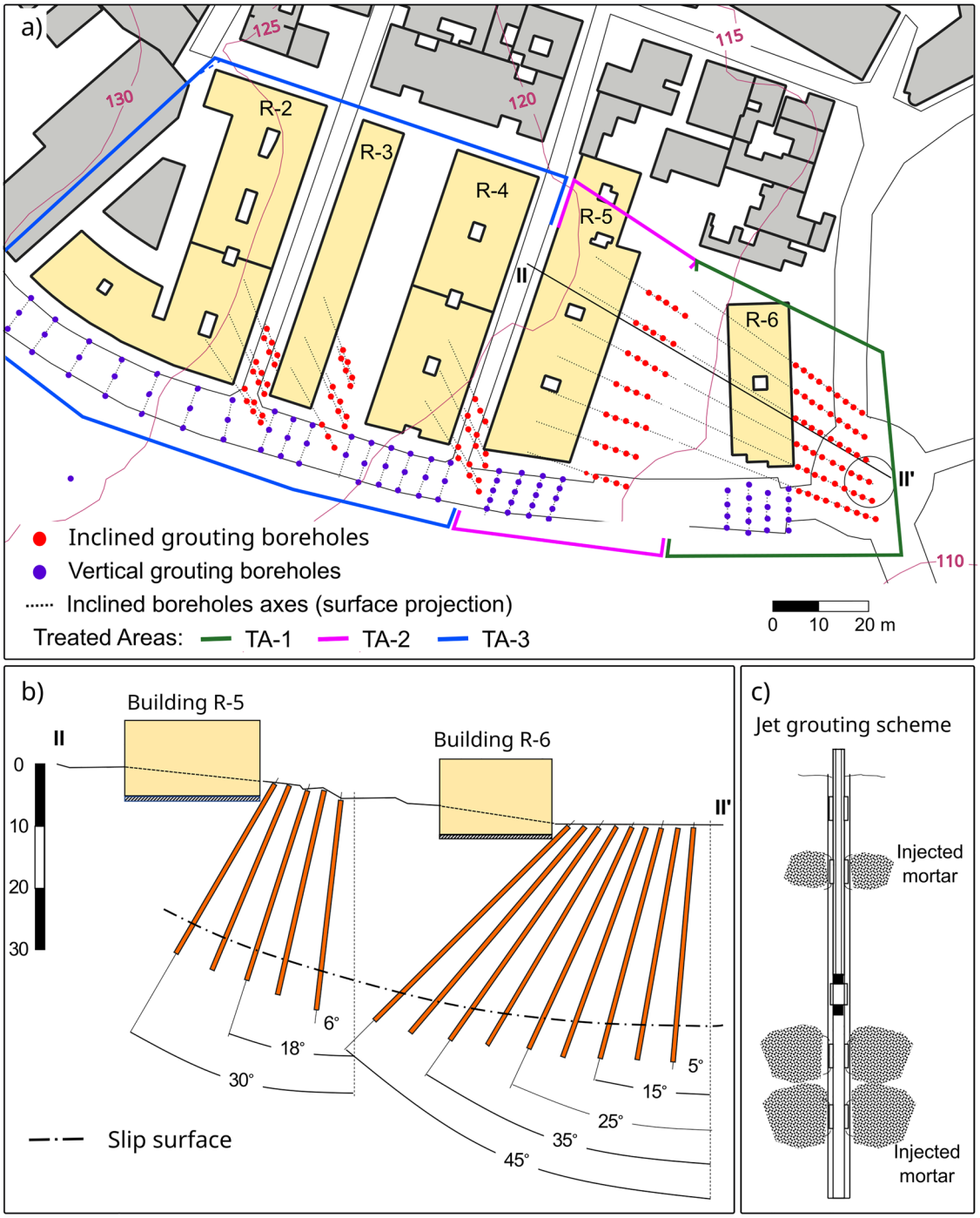

Fig. 5 **a** Map showing the location of the grouting boreholes in La Verbena neighbourhood. **b** Design of the inclined grouting boreholes that intersect the local shear surface (dashed line). **c** Jet grouting scheme

effectiveness of these improvements beyond the head, particularly in the middle part and foot of the slope, remains uncertain due to data limitations. Therefore, while positive effects on the stability of the landslide head are observed, the overall improvement in stability across all regions of the slope cannot be conclusively stated. At the time of writing, the fourth phase had not yet started. It will consist on the underpinning of the foundations of the buildings, improvement and reinforcement of soils, drainage, surface protection, and repair of wet networks, with an estimated cost of 1.5 million €.

InSAR monitoring

Data and processing

We used SAR images acquired by the Sentinel-1 satellite in the Interferometric Wide (IW) swath mode to measure ground movements over the studied area. Two stacks of 172 ascending (track 147) and 179 descending orbit (track 154) acquisitions were processed separately, covering the periods January, 2016–March, 2022, and May, 2016–March, 2022, respectively (Table 2). We limited our analysis to Sentinel-1A (S1A) data having a 12-day repeat cycle. Furthermore, we conducted a more recent InSAR analysis spanning from June, 2022 (coinciding with the completion of the stabilization works), to March, 2023, in both orbits. The list of SAR images is available in Tables TS1, TS2, TS3, and TS4 in the Supplementary Material.

For the data processing we have employed the open source python scripts snap2stamps and the persistent scatterer (PS) method of the StaMPS software package (Hooper et al. 2007, 2004). The snap2stamps scripts operate within the open-source ESA SNAP software, facilitating the automated generation of single reference interferograms from Sentinel-1 data and exporting them to the StaMPS format (Foumelis et al. 2018; Delgado Blasco et al. 2019). The single reference approach involves using one reference SAR image from which all the interferometric pairs are generated. The reference images presented in Table 2 were selected to minimize the dispersion of the perpendicular baseline in each SAR stack as much as possible. To correct the topographic contribution to the radar phase in the interferograms, we used a digital terrain model of the project PNOA-LIDAR (from the National Center of Geographic Information; CNIG) with a resolution cell of 5 m. The StaMPS software package extracts ground deformation data throughout the entire SAR observation period. We have processed a small area of 300 km² in both geometries. StaMPS carries out the initial selection of PS candidates based on the amplitude dispersion (DA), which is defined as the ratio between the standard deviation and mean deviation of the amplitude over time. We chose a DA threshold value of 0.4 to minimize random amplitude variability and exclude pixels exhibiting high temporal decorrelation. The final PS selection is based on a combination of amplitude and estimated phase stability, rejecting those that appear to be persistent only in certain interferograms. After the PS are selected, the PS weeding process drops those that are due to signal contribution from neighbouring ground resolution elements and those deemed too noisy. For the noise-based weeding, we have selected standard deviation values ranging from 0.8 to 1.2 that balances selecting the maximum amount of points with reducing the noise levels. Then, the wrapped phase is corrected for spatially uncorrelated DEM errors. For the phase unwrapping we used the 3-D method (Hooper 2010), which is performed both spatially and temporally. We opted for a short unwrapping time window of 10 or 30 days to prevent irregular trends in the time series caused by reaching extreme values of $-\pi/+\pi$. Additionally, we chose a small unwrapping grid size of 50 m to prevent undersampling of the signal, considering the localized nature of the phenomenon under study and its reduced spatial size. Finally, spatially correlated DEM and orbit errors were estimated and subtracted. A comprehensive description of the StaMPS processing chain steps and its parameterization is provided in the StaMPS/MTI Manual (Hooper et al. 2010). With this analysis we have retrieved the average line-of-sight (LOS) ground deformation rate maps and displacement time series of the four SAR stacks.

Post-processing

We have applied a moving average window of three acquisitions to smooth the displacement time series. In addition, we calculated the 2-D deformation field (eastward and vertical motion) from the PS results combining the two different viewing geometries of the ascending and descending satellite orbit passes, and assuming that the north-south component is negligible. Firstly, we rasterized the PS measuring points of both orbits into a common grid with a pixel size of around 60 × 60 m. Then, we calculated for each pixel the vertical and east-west velocity with the raster calculator tool of the open-source software Q-GIS, using Eqs. (1) and (2) (Béjar-Pizarro et al. 2017),

$$V_{\text{east-west}} = \frac{\left(\frac{vLOS_d}{H_d} - \frac{vLOS_a}{H_a}\right)}{\frac{E_d}{H_d} - \frac{E_a}{H_a}} \quad (1)$$

$$V_{\text{vertical}} = \frac{\left(\frac{vLOS_d}{E_d} - \frac{vLOS_a}{E_a}\right)}{\frac{H_d}{E_d} - \frac{H_a}{E_a}} \quad (2)$$

where

- H_d, H_a = vertical directional cosine of descending and ascending LOS local unit vector;
- E_d, E_a = east–west directional cosine of descending and ascending LOS local unit vector;
- $vLOS_d, vLOS_a$ = mean velocity in the line of sight (LOS) of the descending and ascending satellite orbit modes.

Table 2 Characteristics of the two datasets processed

Satellite	Dataset	Orbit	N. of images	Track	First image	Last image	Years	Ref. image
S1A	1	ASC	172	147	13/05/2016	31/03/2022	5.9	16/04/2019
		DES	179	154	15/01/2016	20/03/2022	6.2	26/10/2019
	2	ASC	51	147	02/06/2021	02/03/2023	1.7	06/01/2022
		DES	51	154	05/06/2021	19/02/2023	1.7	12/02/2022

This approach assumes that, since SAR near-polar orbits cannot effectively detect movements in the north–south direction, there is an absence of ground motion in that particular direction. Since the headings of the ascending and descending tracks are not completely parallel, neglecting the north–south component can result in biased estimates for the east–west and vertical component, making this approach dependent on the actual magnitude of the north–south displacements (Brouwer and Hanssen 2021).

Results

Deformation rate of dataset 1 (January, 2016–March, 2022)

Figure 6 shows the InSAR-derived maps of deformation rates for the 6 years studied period from ascending and descending orbits in the New Town area. The measurements indicate ground displacement along the satellite line of sight (LOS), which has an average value of 45° and 38° from vertical direction for ascending and descending geometries, respectively. Negative and positive values indicate movements away and towards the satellite respectively. Generally, the stability threshold, i.e. the value used to distinguish between areas that are moving and those that are not, is set within a range of 1.5 to 2.0 times the standard deviation of the mean displacement velocity or accumulated displacement in InSAR data from expected stable areas. Therefore, the stability range serves as a measure of processing accuracy and also represents the noise range, defined as the values within which the InSAR technique cannot detect ground displacements. We have established a conservative stability threshold in − 0.4 and 0.4 cm/year based on the standard deviation of the data ($\sigma s \sim 0.18$ cm/year) to assure the significance of the studied displacements. In both geometries the PS are confined to urban areas, and deformation is observed within the boundaries of the landslide head, where the New Town was built (Figs. 6 and S4 in the Supplementary Material). Maximum displacement LOS rates are − 2 cm/year (away) and 1.5 cm/year (towards the satellite). However, these values correspond to the average of the whole processed 6-year period, which contains two differentiated trends as it is shown in the displacement time series (Fig. 9). The maximum values of single PS for the period prior to the deceleration are greater, reaching − 3.8 cm/year in the ascending orbit and 2.7 cm/year in the descending. The magnitude and spatial distribution of the deformation are similar in both geometries, increasing towards the west of the landslide's head.

Figure 7 shows the mean velocity maps for the vertical and horizontal (E-W) components, projected from the S-1 ascending and descending datasets. The vertical projection of the deformation (Fig. 7a) shows subsidence below the main scarp at the eastern part of the head of the landslide with a maximum magnitude of − 0.93 cm/year for the whole 2016–2022 period. The horizontal projection shows that the head of the landslide moves towards the east with rates reaching 2.5 cm/year. These results emphasize that the horizontal component is dominant.

Deformation rate of dataset 2 (June, 2021–March, 2023)

Figure 8 shows the InSAR-derived maps of deformation rates for the June, 2021–March, 2023, time span, from ascending and descending orbits in the New Town area located at the landslide head. We have used the same LOS velocity colour scale as in Fig. 6 for the sake of comparison. The results show a drastic reduction of the deformation in comparison to the other processed dataset. Maximum displacement LOS rates are − 1.2 cm/year (away) and 0.8 cm/year (towards). The PS density is higher around buildings R-5 and R-6. In the ascending orbit, it can be seen how the deformation is greater in the southern part area of building R-6 than in the northern one.

Deformation time series

In Fig. 9 we have plotted the average LOS displacement time series of all the PS contained within the head of the landslide for both geometries. This choice was made because, despite the heterogeneous magnitudes of movement, the temporal behaviour

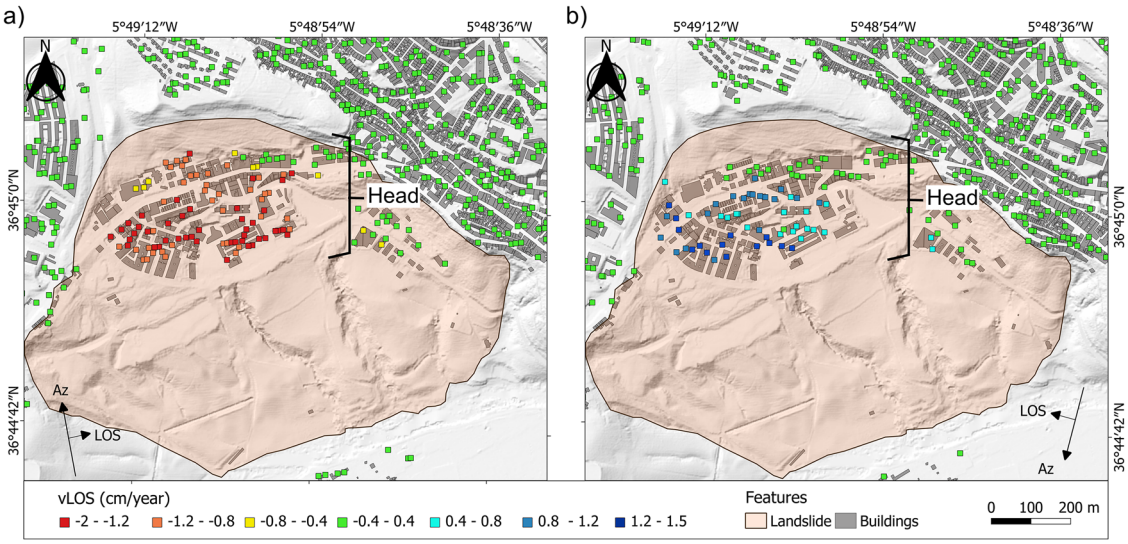

Fig. 6 Mean velocity in LOS for the period 2016–2022 (dataset 1) obtained from **a** ascending orbit and **b** descending orbit

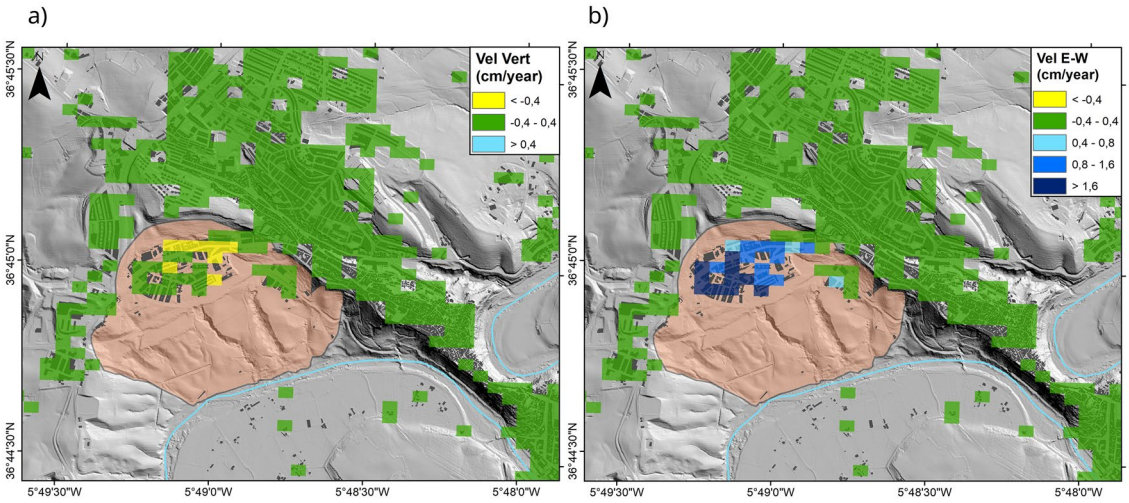

Fig. 7 Mean velocity maps for the **a** vertical and **b** horizontal components for the period 2016–2022 (dataset 1), projected from the S-1 ascending and descending orbits

is consistent across all PS in the landslide head (see Fig. S5 in the Supplementary Material). Datasets 1 and 2 are presented together, overlapping for the time span from June, 2021, to March, 2022. We have smoothed the time series using a moving average window of three acquisitions. The total displacement is greater in the ascending LOS direction, reaching 7 cm of deformation away from the satellite; meanwhile, in the descending LOS direction, the total displacement is 4.5 cm towards the satellite. The trend of both time series changes around the mid-end of 2018, showing an unambiguous deceleration of the landslide head. We applied an automated classification method proposed by Berti et al. (2013) to categorize PS. Those above the stability threshold within the landslide head display a bilinear or discontinuous behaviour in their time series. This behaviour is characterized by two linear tracts of different velocities separated by a break point, consistently indicating deceleration. The average time series (Fig. 9) reveals a break point date of November, 2018, for the ascending orbit and May, 2018, for the descending orbit. Before the break point, the mean LOS velocity of the landslide head, computed by bilinear regression, is − 2.2 cm/year in the ascending orbit (movement away from the satellite) and 1.3 cm/year in the descending orbit (towards the satellite). After this date, the velocity decreases to − 0.43 cm/year and 0.23 cm/year, respectively. Notably, the time series of dataset 2 shows a strong correlation with dataset 1 in the overlapping period and continues with a similar trend.

Discussion

Ground deformation

The Arcos de la Frontera landslide occurs in an environmental setting that presents some challenges to InSAR techniques, particularly related to land cover and slope orientation. The PS in the LOS velocity maps (Figs. 6 and 8) are confined to the urban area, as there are no natural targets with stable scattering

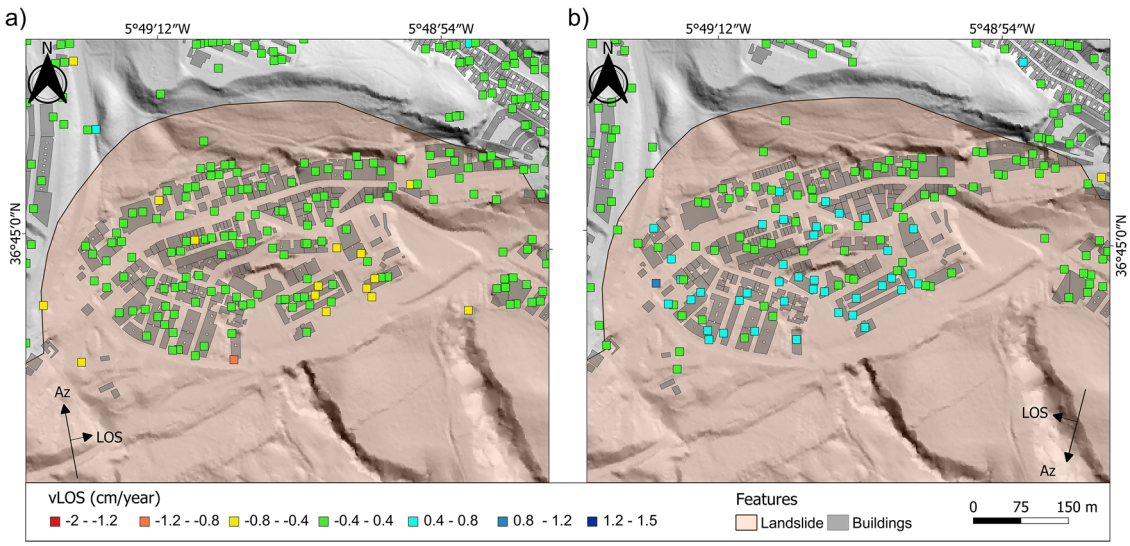

Fig. 8 **a** Mean velocity in LOS obtained from the ascending orbit for the period 2021–2023 (dataset 2) of the landslide head. **b** Mean velocity in LOS obtained from the descending orbit for the period 2021–2023 (dataset 2) of the landslide head

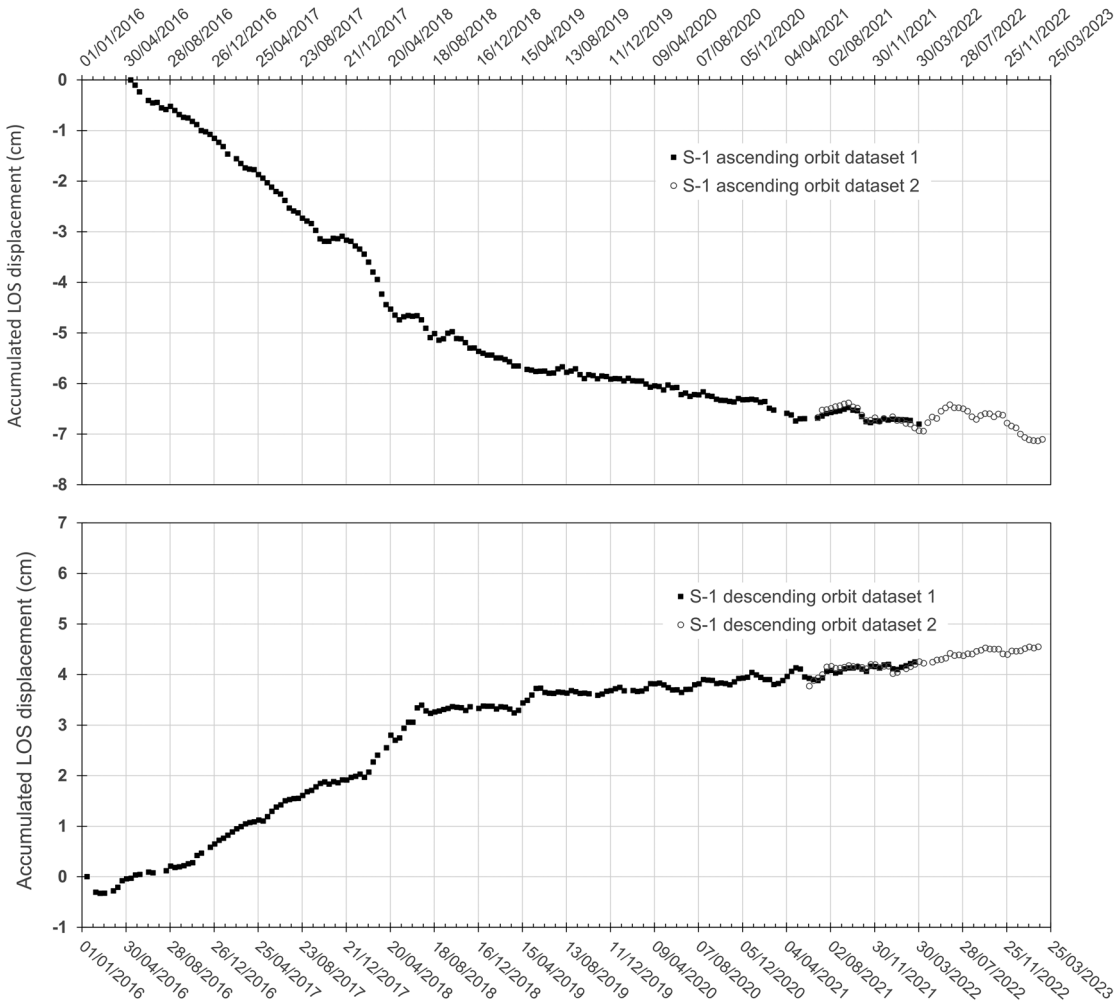

Fig. 9 Average LOS displacement TS of all the PS contained within the landslide head area in ascending and descending orbits

properties on the slope covered by low herbs and shrub vegetation (e.g. Wasowski and Pisano 2020). Consequently, the StaMPS method using C-band data does not detect features in this specific terrain, preventing us from obtaining information about the dynamics of the middle and the foot of the landslide. However, the urbanized head of the landslide shows a high PS density providing spatially extensive information (e.g. Bianchini et al. 2015; Guerriero et al. 2021). The LOS velocity maps in both orbits and displacement TS (Fig. 7) clearly highlight that the head of the landslide was active with LOS rates of more than 2 cm/year at least until mid-2018, in accordance to previous works (Béjar-Pizarro et al. 2017; Bru et al. 2017). During the initial InSAR period (2016–2022), no PS was identified in the vicinity of buildings R-5 and R-6. This absence could be attributed to the gradual deterioration of urban elements, including pavement, stairs, and walls, as well as vegetation growth around these structures due to a lack of maintenance in the studied period. These ground surface modifications become evident when examining photographs taken between 2009 and 2022 (see Fig. S6 in the Supplementary Material). Such alterations can lead to changes in the scattering characteristics of the terrain between two consecutive SAR acquisitions, causing temporal decorrelation—a key factor driving coherence loss (Hanssen 2001). In the StaMPS algorithm, PS candidates are selected based on the temporal coherence of nearby pixels; therefore, the high temporal decorrelation of the pixels surrounding the building could hinder their selection at that site. We tried less restrictive values of initial D_A and weeding thresholds, but there were not selected PS in that location in any case. The opposite LOS directions between orbits indicate a strong horizontal component. It is crucial to acknowledge the non-homogeneous direction of motion at the head of the landslide, influenced by factors such as the maximum local slope and shear surface. For instance, in the western part of the landslide head, cracks in the pavement and tachymeter surveys indicate a motion direction of 330°NE around building R-6, which transitions to about 280°NE uphill La Verbena. However, in the eastern part of the landslide head, the local slope and the orientation of cracks in the buildings beneath the main scarp suggest a significant N-S component in that area (refer to Fig. 10). Importantly, SAR satellites with quasi-polar orbits are insensitive to N-S motion, limiting the deformation analysis derived from such data in these areas. These directional limitations in the satellite data could lead to biases in the interpretation of both vertical and horizontal movements in

the scarp area. The insensitivity to N-S motion means that the full extent of deformation, particularly in the eastern part of the landslide head, might not be accurately captured. Consequently, the analysis may underestimate the true magnitude and nature of deformation in these specific regions (Brouwer and Hanssen 2021). Anyhow, the vertical projection of the deformation with the selected approach (Fig. 8a) highlights subsidence below the main scarp at the eastern part of the head of the landslide for the first studied period, remarkably reducing its magnitude after mid-2018. The horizontal E-W projection (Fig. 8b) assumes all the horizontal movement is along this direction, which is identified in the western part of the head of the landslide and La Verbena neighbourhood, but is not observed throughout the entire head of the landslide. The discrepancy in the maximum horizontal projected values for the studied period, being situated at the northwest rather than in La Verbena as indicated in prior studies (Béjar-Pizarro et al. 2017; Bru et al. 2017), can be attributed to the absence of persistent scatterers (PS) near buildings R-5 and R-6, which obscures the movement in that area. The southern part of building R-6 exhibits a movement direction of 330°NE, indicating that the purely horizontal E-W projection underestimates the real displacement magnitude.

The displacement TS have a similar trend in both geometries, showing a deceleration after mid-2018. This behaviour is common to all the PS of the landslide head, stressing that although the direction of movement is heterogeneous, the deceleration occurred in the entire landslide head. The average LOS velocity of all the PS within the landslide head in the ascending orbit during the first period (from early 2016 to mid-2018) exceeds 2 cm/year and subsequently decreases to values close to the stability threshold. The maximum values of single PS for the period prior to the deceleration are greater, reaching 3.8 cm/year in the LOS ascending orbit. The deformation rate magnitude recorded in the first period is in concordance with previous InSAR studies. We have also compared the LOS velocities with the European Ground Motion Service (EGMS) products showing a very good agreement for both geometries. In Fig. 11 we have plotted the average landslide head descending LOS time series of the Envisat results from April, 2011, to February, 2012 (Bru et al. 2017), with the Sentinel-1 results from the EGMS calibrated product (https://egms.land.copernicus.eu/) and our StaMPS results for the period 2016–2023. Assuming a constant rate for the non-data period, we can estimate a total LOS displacement of more than 10 cm for the period 2011–2023.

The reason to process the second period of June, 2021, to March, 2023, was to retrieve information of the current situation in the landslide head after the end of the local stabilization works. Being a shorter period and therefore reducing the temporal decorrelation effect, PS could be detected at the location of the most affected buildings, R-5 and R-6. Although the deformation in this period is drastically reduced compared to the previous mid-2018, the ascending orbit clearly captures a differential movement of building R-6, which indicates that the tilting process is still active. However, we cannot determine if the ongoing tilting is caused by the soil

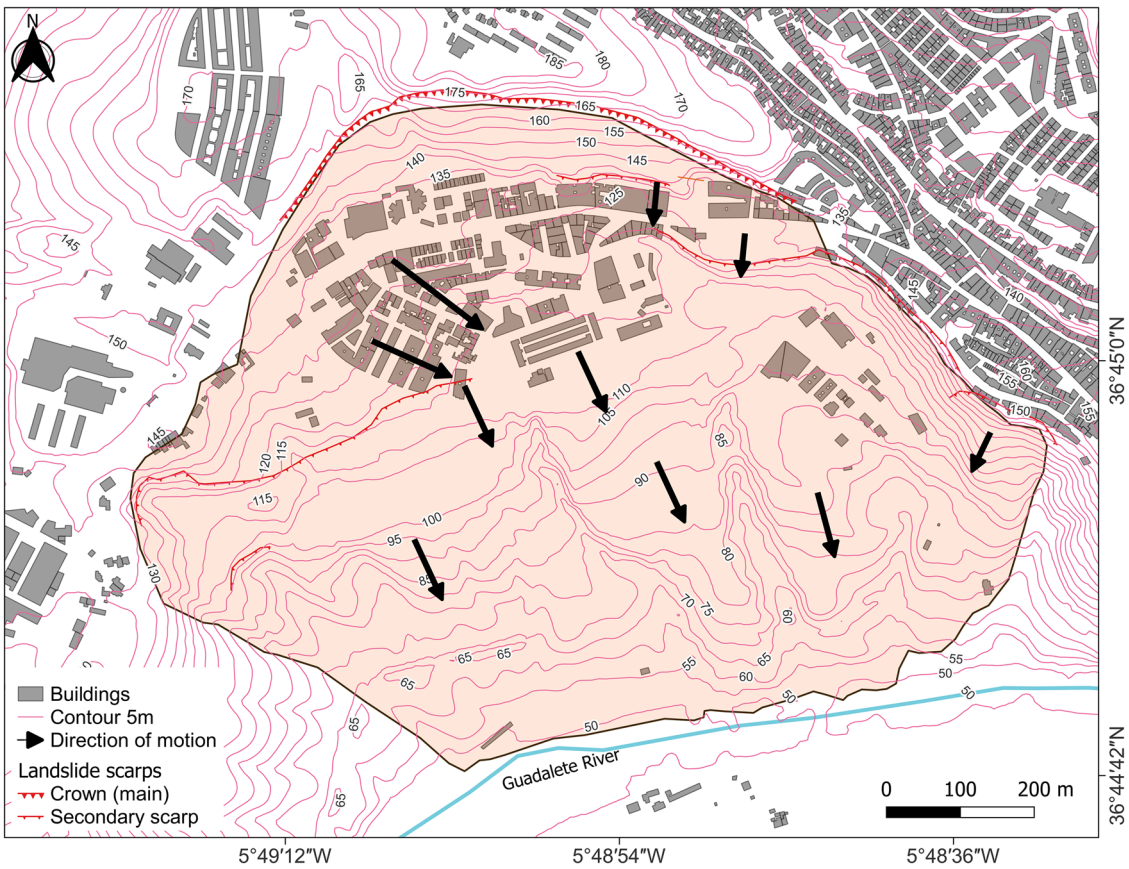

Fig. 10 Interpreted directions of motion at the landslide

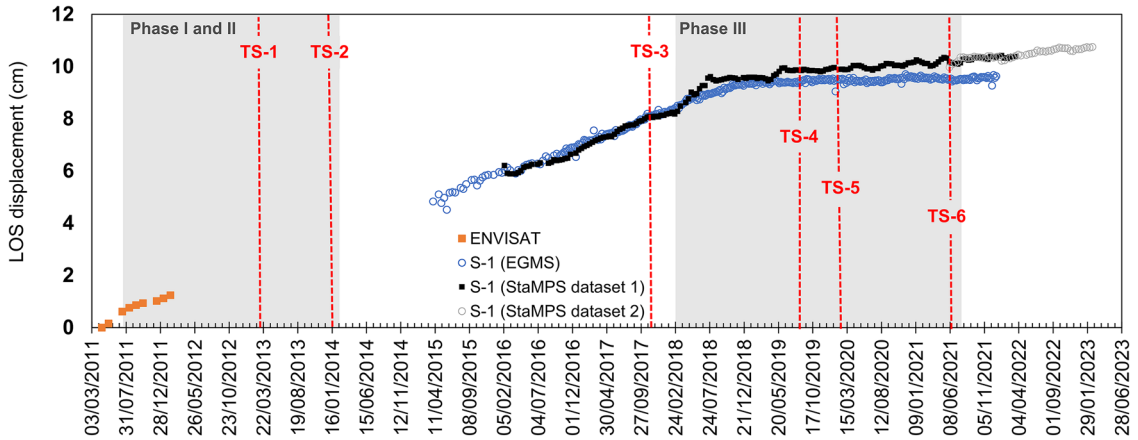

Fig. 11 Average descending LOS time series of all the PS within the landslide head from the Envisat satellite (Bru et al. 2017) and the Sentinel-1 satellite, from the EGMS-calibrated product and the StaMPS datasets processed in this work (descending orbits). The dashed red lines indicate the dates of the tachymeter surveys. The three phases of local stabilization works are also illustrated

movement or due to the failure of the foundation itself. In any case, the TS of this more recent period underscores that the movement is ongoing at extremely low rates.

InSAR results versus local stabilization works and in situ measurements

In terms of comparing the InSAR results with the stabilization works, a noteworthy observation is that the change in the time series (TS) trend is consistent across all persistent scatterers (PS) above the stability threshold, suggesting a uniform deceleration of deformation behaviour throughout the entire head of the landslide. This implies that the local stabilization works conducted in La Verbena neighbourhood have effectively stabilized the entire landslide head. Nevertheless, the absence of InSAR information in the middle part and foot of the landslide prevents us from determining if the local stabilization works have influenced these regions. During our field inspection at the end of 2022, we observed ongoing shallow movement phenomena, such as creeping. We have dismissed the idea that there is a relationship between the deceleration of the head of the landslide and the rainfall rates during the studied period by InSAR. The graphs in Fig. S7 of the Supplementary Material display the average line-of-sight (LOS) displacements (TS) of all the PS within the landslide head area (in both ascending and descending orbits), along with accumulated monthly rainfall data. The distribution of monthly precipitation varies over the years, but in terms of total accumulated rainfall, the years 2019–2023 are not drier than the period 2015–2017 (Fig. S8 in the Supplementary Material). Nevertheless, an acceleration of the landslide head movement is observed in both geometries around March, 2018, when the accumulated rainfall surpassed 350 mm. Another peak in rainfall occurred in December, 2022, exceeding 250 mm, resulting in a slight acceleration only appreciable in the ascending orbit. Prior to the time interval studied with InSAR, there was another period of intense rainfall in December, 2009, and February, 2010, with monthly peaks of accumulated rainfall exceeding 330 mm. This event caused a 5-m rise in the groundwater table, which was being measured at that time, and led to an increase in reported urban damages (Bru et al. 2017). The potential mechanism behind the observed acceleration during periods of higher rainfall is the gradual reduction in suction on the sliding clayey materials. This reduction can decrease the effective stress and strength, consequently compromising slope stability (López-Vinielles et al. 2020). These observations suggest that the landslide reacts to rainfall, but the stabilization of the landslide head is attributed to the improvement of geotechnical properties of soil through the jet grouting works rather than a reduction in average precipitation.

We made a comparison between our InSAR results and the outcomes of the technical report on the monitoring of movements using tachymeter surveys (Cobo 2021). The InSAR results show that the phases I and II of the local stabilization works performed between 2011 and 2014 were not effective to stop the head landslide motion. In 2014, the second tachymeter survey (TS-2 in Fig. 11), conducted when there is no InSAR data, suggested that the motion had ceased. However, the third survey in 2017 (TS-3) revealed a reactivation of motion in the treated area TA-3, corresponding to the location of buildings R-2, R-3, and R-4 (Fig. 5). Subsequently, in February, 2018, phase III commenced. The InSAR results demonstrate that the drainage and injections started becoming effective between the mid- and end of 2018. Tachymeter surveys in August, 2019, and February, 2020 (TS-4 and TS-5, respectively) identified a reactivation of adverse movements in the treated areas TA-1 and TA-2, although InSAR monitoring did not capture them. It must be considered that the tachymeter information we handle is limited to the direction of motion, but we lack quantitative measurements. In the June, 2021, survey (TS-6), movement in the treated area TA-2 had begun to reverse, while no movement was detected in TA-1 and TA-3. However, descending InSAR results for the period of 2021–2023 reveal extremely slow movement in the eastern area of La Verbena, indicating the possibility of ongoing motion in these regions. Furthermore, the technical report on the monitoring of movements using tachymeter surveys suggests that movements could persist until the repair of foundations and urbanization is complete.

Conclusion

In this study, we used InSAR products to perform a long-term motion analysis of a slow-moving planar slide earthflow in Arcos de la Frontera (Spain), a phenomenon causing significant urban damages. Our primary objective was to assess the effectiveness of local stabilization works, which involved draining the western part of the slope head and implementing jet grouting via boreholes to improve both bearing capacity and relative density of the ground in La Verbena neighbourhood area. The results are significant, demonstrating that the local stabilization works in La Verbena neighbourhood have effectively stabilized the entire head of the landslide and influenced a much larger area beyond the zone of the local interventions. However, it is crucial to acknowledge that the assessment of the improvements in the middle part and foot of the slope remains uncertain due to limitations in InSAR data. Therefore, while positive effects on the stability of the landslide head are observed, we cannot conclusively state an overall improvement in stability across all regions of the slope.

We made a comprehensive review of historical and recent urban damages attributed to the landslide motion. The background of this slope instability highlights the need for geological risk studies prior to urban development plans. We conducted on-site field assessments to document the current state of urban damages and geomorphological features. We also described the local stabilization works undertaken and compared the in-situ tachymetry surveys with our InSAR data. We have generated mean line-of-sight (LOS) velocity maps and displacement time series using Sentinel-1 SAR images in both ascending and descending orbits, covering a period exceeding 7 years (from 2016 to 2023) divided into two periods. The displacement time series from both orbits exhibit a deceleration of the entire landslide head after mid-2018. The vertical projection of the deformation highlights significant activity beneath the main scarp until mid-2018. The analysis of the second SAR dataset indicates that the landslide remains active, albeit with an extremely slow velocity.

The use of InSAR has contributed to have an improved spatial picture of the displacements in this site, supplying data outside the in-situ monitoring area and adding valuable information of the stabilization work effects. Our results reinforce the advantages of implementing InSAR techniques as a complementary tool to geotechnical monitoring. The X-band data provided by commercial satellites with finer resolution (such as StripMap COSMO-Skymed with a spatial resolution of 3×3 m), coupled with the application of a purely PS InSAR method, would likely enhance the measurements of the urbanized area. However, it is remarkable that the use of medium-resolution S1 C-band SAR data has produced valuable results. The accessibility of free historic S1 data, consistent revisit times, and the upcoming S1-C mission with increased data frequency make it a versatile option for geotechnical monitoring in slow-moving landslides, with natural or man-made reflectors and adequate slope orientation. The implementation of an operational real-time geotechnical monitoring with InSAR is challenging, but obtaining up to date data every few months is feasible using local processors or cloud-based solutions (such as the Geohazard Exploitation Platform funded by ESA). This could prevent important changes of displacement rates at a competitive cost, with better spatial resolution and enlarged areas than other in situ monitoring techniques.

Acknowledgements

We would like to thank Alejandro A. Cobo Fernández for providing the jet grouting locations, tachymeter survey information, and cross-hole seismic pair data, as well as the personal communications.

Funding

This work was supported by project UNDERGY, subsidized by the Center for Industrial Technological Development (CDTI), within the framework of the Recovery, Transformation and Resilience Plan and the State Program for Business Leadership in R&D&I, of the State Plan for Scientific and Technical Research and Innovation 2021–2023, and project PID2020-116540RB-C22 funded by MCIN/AEI/10.13039/501100011033 and project EGMS RASTOOL: European ground motion risk assessment tool (Grant Agreement No. 101048474) funded by the European Commission, Directorate-General Humanitarian Aid and Civil Protection (ECHO).

Data availability

Data sets generated during the current study are available from the corresponding author on reasonable request. EGMS data is available at https://egms.land.copernicus.eu/.

Declarations

Conflict of interest The authors declare no competing interests.

References

Alonso E, Gens A (2006) Aznalcollar dam failure. Part 1: Field observations and material properties. Géotechnique 56(3):165–183. https://doi.org/10.1680/geot.2006.56.3.165

Béjar-Pizarro M, Notti D, Mateos RM, Ezquerro P, Centolanza G, Herrera G, Bru G, Sanabria M, Solari L, Duro J (2017) Mapping vulnerable urban areas affected by slow-moving landslides using Sentinel-1 InSAR data. Remote Sensing 9(9):876. https://doi.org/10.3390/rs9090876

Berti M, Corsini A, Franceschini S, Iannacone JP (2013) Automated classification of Persistent Scatterers Interferometry time series. Nat Hazards Earth Syst Sci 13(8):1945–1958. https://doi.org/10.5194/nhess-13-1945-2013

Bianchini S, Ciampalini A, Raspini F, Bardi F, Di Traglia F, Moretti S, Casagli N (2015) Multi-temporal evaluation of landslide movements and impacts on buildings in San Fratello (Italy) by means of C-band and X-band PSI data. Pure Appl Geophys 172:3043–3065. https://doi.org/10.1007/s00024-014-0839-2

BOE (2011a) BOE-A-2011-3258. Boletín Oficial del Estado (Official State Gazette, in Spanish). https://www.boe.es/diario_boe/txt.php?id=BOE-A-2011-3258. Accessed 5 Apr 2023

BOE (2011b) BOE-A-2011-17563. Boletín Oficial del Estado (Official State Gazette, in Spanish). https://www.boe.es/eli/es/rd/2011/11/04/1601. Accessed 5 Apr 2023

Brouwer WS, Hanssen RF (2021) An analysis of Insar displacement vector decomposition fallacies and the strap-down solution. Proceedings of IEEE International Geoscience and Remote Sensing Symposium IGARSS2021, IEEE, p. 2927–2930. https://doi.org/10.1109/IGARSS47720.2021.9554216

Bru G, González PJ, Mateos RM, Roldán FJ, Herrera G, Béjar-Pizarro M, Fernández J (2017) A-DInSAR monitoring of landslide and subsidence activity: a case of urban damage in Arcos de la Frontera. Spain Remote Sensing 9(8):787. https://doi.org/10.3390/rs9080787

Bru G, Escayo J, Fernández J, Mallorqui JJ, Iglesias R, Sansosti E, Abajo T, Morales A (2018) Suitability assessment of X-band satellite SAR data for geotechnical monitoring of site scale slow moving landslides. Remote Sensing 10(6):936. https://doi.org/10.3390/rs10060936

Ciampalini A, Farina P, Lombardi L, Nocentini M, Taurino V, Guidi R, Pina F, Tavarini D (2021) Integration of satellite InSAR with a wireless network of geotechnical sensors for slope monitoring in urban areas. The Pariana Landslide Case (Massa, Italy). Remote Sens 13(13):2534. https://doi.org/10.3390/rs13132534

Cigna F, Tapete D (2021) Sentinel-1 BigData processing with P-SBAS InSAR in the geohazards exploitation platform: an experiment on coastal land subsidence and landslides in Italy. Remote Sens 13(5):885. https://doi.org/10.3390/rs13050885

Cigna F, Banks VJ, Donald AW, Donohue S, Graham C, Hughes D, McKinley JM, Parker K (2017) Mapping ground instability in areas of geotechnical infrastructure using satellite InSAR and Small UAV surveying: a case study in Northern Ireland. Geosciences 7(3):51. https://doi.org/10.3390/geosciences7030051

CLMS (2023) European Ground Motion Service Technical Summary. https://land.copernicus.eu/en/products/european-ground-motion-service. Accessed 30 Dec 2023

Cobo AA (2021) Proyecto de ejecución final de las obras de emergencia complementarias para la estabilización parcial de la zona correspondiente a la urbanización "La Verbena" de Arcos de la Frontera (Cádiz) - fase 3.2 (technical report, in Spanish)

Colesanti C, Wasowski J (2006) Investigating landslides with space-borne Synthetic Aperture Radar (SAR) interferometry. Eng Geol 88(3–4):173–199. https://doi.org/10.1016/j.enggeo.2006.09.013

Confuorto P, Di Martire D, Infante D, Novellino A, Papa R, Calcaterra D, Ramondini M (2019) Monitoring of remedial works performance on landslide-affected areas through ground-and satellite-based techniques. CATENA 178:77–89. https://doi.org/10.1016/j.catena.2019.03.005

Cook ME, Brook MS, Hamling IJ, Cave M, Tunnicliffe JF, Holley R (2023) Investigating slow-moving shallow soil landslides using Sentinel-1 InSAR data in Gisborne. New Zealand Landslides 20(2):427–446. https://doi.org/10.1007/s10346-022-01982-9

Costantini M, Minati F, Trillo F, Ferretti A, Passera E, Rucci A, Dehls J, Larsen Y, Marinkovic P, Eineder M (2022) EGMS: Europe-wide ground motion monitoring based on full resolution InSAR processing of all Sentinel-1 acquisitions. In: Proceedings IGARSS 2022–2022 IEEE International Geoscience and Remote Sensing Symposium 2022, IEEE, p. 5093–5096. https://doi.org/10.1109/IGARSS46834.2022.9884966

Czikhardt R, Papco J, Bakon M, Liscak P, Ondrejka P, Zlocha M (2017) Ground stability monitoring of undermined and landslide prone areas by means of sentinel-1 multi-temporal InSAR, case study from Slovakia. Geosciences 7(3):87. https://doi.org/10.3390/geosciences7030087

Del Soldato M, Riquelme A, Bianchini S, Tomás R, Di Martire D, De Vita P, Moretti S, Calcaterra D (2018) Multisource data integration to investigate one century of evolution for the Agnone landslide (Molise, southern Italy). Landslides 15:2113–2128. https://doi.org/10.1007/s10346-018-1015-z

Delgado Blasco JM, Foumelis M, Stewart C, Hooper A (2019) Measuring urban subsidence in the Rome metropolitan area (Italy) with Sentinel-1 SNAP-StaMPS persistent scatterer interferometry. Remote Sensing 11(2):129. https://doi.org/10.3390/rs11020129

Di Maio C, Fornaro G, Gioia D, Reale D, Schiattarella M, Vassallo R (2018) In situ and satellite long-term monitoring of the Latronico landslide, Italy: displacement evolution, damage to buildings, and effectiveness of remedial works. Eng Geol 245:218–235. https://doi.org/10.1016/j.enggeo.2018.08.017

Dictum (2014) Court ruling N° 153 / 2014. Audiencia Provincial de Jerez de la Frontera. Nº de Recurso: 24/2014. https://www.poderjudicial.es/search/AN/openDocument/a6bd4d0a0f5e60d2/20150224

Dunnicliff J (1993) Geotechnical instrumentation for monitoring field performance. John Wiley & Sons, New York

EDARTEC (2009) Informe de visita de reconocimiento e inspección nº3 (technical report, in Spanish)

Escolano Sánchez F, Bueno Aguado M, Melentijevic S (2019) Stress-strain behavior of blue marls from the Guadalquivir river basin in Spain. Acta Geotechnica Slovenica 16(1):30–42

EXPERTA (2009) Informe sobre el estudio de patologías existentes, control de movimiento de fisuras y control de desplomes en edificios de viviendas en Pz. Ayuntamientos democráticos nº2 y nº4. Arcos de la Frontera, Cádiz (technical report, in Spanish)

Foumelis M, Delgado Blasco JM, Desnos Y-L, Engdahl M, Fernandez D, Veci L, Lu J, Wong C (2018) ESA SNAP - StaMPS integrated processing for Sentinel-1 persistent scatterer interferometry. Proceedings of IEEE International Geoscience and Remote Sensing Symposium, pp. 1364–1367. https://doi.org/10.1109/IGARSS.2018.8519545

García A (1970) Informe geológico sobre el terreno afectado por el Canal de Tablellina (PK 1461 a PK 3434). Término municipal de Arcos de la Frontera (Cádiz): Servicio Geológico de Obras Públicas (technical report, in Spanish)

Guerriero L, Confuorto P, Calcaterra D, Guadagno FM, Revellino P, Di Martire D (2019) PS-driven inventory of town-damaging landslides in the Benevento, Avellino and Salerno Provinces, southern Italy. J Maps 15(2):619–625. https://doi.org/10.1080/17445647.2019.1651770

Guerriero L, Prinzi EP, Calcaterra D, Ciarcia S, Di Martire D, Guadagno FM, Ruzza G, Revellino P (2021) Kinematics and geologic control of the deep-seated landslide affecting the historic center of Buonalbergo, southern Italy. Geomorphology 394:107961. https://doi.org/10.1016/j.geomorph.2021.107961

Guilhot D, Hoyo TM, Bartoli A, Ramakrishnan P, Leemans G, Houtepen M, Salzer J, Metzger JS, Maknavicius G (2021) Internet-of-things-based geotechnical monitoring boosted by satellite InSAR data. Remote Sensing 13(14):2757. https://doi.org/10.3390/rs13142757

Hanssen RF (2001) Radar interferometry: data interpretation and error analysis. Springer Science & Business Media. https://doi.org/10.1007/0-306-47633-9

Herrera G, Gutiérrez F, García-Davalillo J, Guerrero J, Notti D, Galve J, Fernández-Merodo J, Cooksley G (2013) Multi-sensor advanced DInSAR monitoring of very slow landslides: the Tena Valley case study (Central Spanish Pyrenees). Remote Sens Environ 128:31–43. https://doi.org/10.1016/j.rse.2012.09.020

Hilley GE, Bürgmann R, Ferretti A, Novali F, Rocca F (2004) Dynamics of slow-moving landslides from permanent scatterer analysis. Science 304(5679):1952–1955. https://doi.org/10.1126/science.1098821

Hooper A (2008) A multi-temporal InSAR method incorporating both persistent scatterer and small baseline approaches. Geophys Res Lett. https://doi.org/10.1029/2008GL034654

Hooper A (2010) A statistical-cost approach to unwrapping the phase of InSAR time series. ESA Special Publication, pp. 59–63. https://ui.adsabs.harvard.edu/abs/2010ESASP.677E..59H

Hooper A, Zebker H, Segall P, Kampes B (2004) A new method for measuring deformation on volcanoes and other natural terrains using InSAR persistent scatterers. Geophys Res Lett. https://doi.org/10.1029/2004GL021737
Hooper A, Segall P, Zebker H (2007) Persistent scatterer interferometric synthetic aperture radar for crustal deformation analysis, with application to Volcán Alcedo. J Geophys Res, Galápagos. https://doi.org/10.1029/2006JB004763
Hooper A, Spaans K, Bekaert D, Cuenca MC, Arıkan M, Oyen A (2010) StaMPS/MTI manual: Delft Institute of Earth Observation and Space Systems Delft University of Technology. Kluyverweg 1:2629
Hungr O, Leroueil S, Picarelli L (2014) The Varnes classification of landslide types, an update. Landslides 11(2):167. https://doi.org/10.1007/s10346-013-0436-y
Kalia AC (2023) Landslide activity detection based on Sentinel-1 PSI datasets of the Ground Motion Service Germany—the Trittenheim case study. Landslides 20(1):209–221. https://doi.org/10.1007/s10346-022-01958-9
Liu S, Segoni S, Raspini F, Yin K, Zhou C, Zhang Y, Casagli N (2020) Satellite InSAR as a new tool for the verification of landslide engineering remedial works at the regional scale: a case study in the Three Gorges Resevoir Area. China Applied Sciences 10(18):6435. https://doi.org/10.3390/app10186435
López-Vinielles J, Ezquerro P, Fernández-Merodo JA, Béjar-Pizarro M, Monserrat O, Barra A, Blanco P, García-Robles J, Filatov A, García-Davalillo JC (2020) Remote analysis of an open-pit slope failure: Las Cruces case study, Spain. Landslides 17:2173–2188. https://doi.org/10.1007/s10346-020-01413-7
Mantovani F, Soeters R, Van Westen C (1996) Remote sensing techniques for landslide studies and hazard zonation in Europe. Geomorphology 15(3–4):213–225. https://doi.org/10.1016/0169-555X(95)00071-C
MCH (2009) Informe pericial. Daños en el edificio de viviendas y garajes "La Verbena R6". MCH arquitectos. Expediente 09.005 (technical report, in Spanish)
Minh DHT, Hanssen R, Rocca F (2020) Radar interferometry: 20 years of development in time series techniques and future perspectives. Remote Sens 12(9):1364. https://doi.org/10.3390/rs12091364
Moncloa (2017) Consejo de Ministros (Spanish Minister council) Referencia 20 de octubre de 2017. https://www.lamoncloa.gob.es/consejodeministros/referencias/documents/2017/refc20171020.pdf (in Spanish)
Osmanoğlu B, Sunar F, Wdowinski S, Cabral-Cano E (2016) Time series analysis of InSAR data: methods and trends. ISPRS J Photogramm Remote Sens 115:90–102. https://doi.org/10.1016/j.isprsjprs.2015.10.003
Oteo CS (2000) Las margas azules del Guadalquivir y la inestabilidad de taludes. Rutas: Revista de la Asociación Técnica de Carreteras, no. 77, p. 17–27 (in Spanish). http://www.atc-piarc.com/rutas_historico.php?rID=114&pagb=&ky=2000. Accessed 5 May 2023
PGOU (1995) Plan General de Ordenación Urbana del Ayuntamiento de Arcos de la Frontera. Cádiz (technical report, in Spanish). https://pgouarcos.es/?page_id=77. Accessed 31 Apr 2023
Sandwell D, Mellors R, Tong X, Wei M, Wessel P (2011) Open radar interferometry software for mapping surface deformation. Eos Trans 92(28):234–235. https://doi.org/10.1029/2011EO280002. American Geophysical Union
Sanz de Galdeano C, Vera JA (1992) Una propuesta de clasificación de las cuencas neógenas béticas. Acta Geológica Hispánica 26(3–4):205–227 (in Spanish)
Solari L, Del Soldato M, Raspini F, Barra A, Bianchini S, Confuorto P, Casagli N, Crosetto M (2020) Review of satellite interferometry for landslide detection in Italy. Remote Sens 12(8):1351. https://doi.org/10.3390/rs12081351
TEDECO (2000) Estudio Geotécnoco. Peticionarios: ARMENDARIZ E.C S.A. y GESTORIA BAJA MAR S.L. Solar: Parcelas R-3, R-4, R-5 y R-6 de la UE-11 La Verbena. Arcos de la Frontera, Cádiz (technical report, in Spanish)
Tsige M, Corral M (2013) Ángulo Estable y Tratamientos y Mejora de Taludes en las Arcillas Azules del Guadalquivir (AAG). VIII Simposio Nacional Sobre Taludes y Laderas Inestables, CIMNE, Barcelona, 3:997–1008, ISBN 978-84-941407-1-6 (in Spanish)
Tsige M, de Vallejo LG, Doval M, Oteo C, Barba C (1995) Microfabric of Guadalquivir blue marls and its engineering geological significance. Proceedings of Int. Assoc. of Engineering Geology, pp 659–665
Uriel S, Fornes J (1994) Back-analysis of a landslide in overconsolidated tertiary clays of the Guadalquivir River valley. Proceedings of Int. conference on soil mechanics and foundation engineering, pp 1099–1102
Uriel S, Oteo C (1976) Propiedades Geotécnicas de las Margas azules de Sevilla. Proceedings of Simposium Nacional sobre Rocas Blandas. Madrid, v. 1 (in Spanish)
VORSEVI (2003) Reconocimiento geotécnico. Estabilización desmonte bajo escuela taller y plataforma en recinto ferial (technical report, in Spanish)
VORSEVI (2009) Reconocimiento geotécnico UE "La Verbena" (technical report, in Spanish)
VORSEVI (2010) Reconocimiento geotécnico UE "La Verbena" (technical report, in Spanish)
Wasowski J, Bovenga F (2014) Investigating landslides and unstable slopes with satellite Multi Temporal Interferometry: Current issues and future perspectives. Eng Geol 174:103–138. https://doi.org/10.1016/j.enggeo.2014.03.003
Wasowski J, Pisano L (2020) Long-term InSAR, borehole inclinometer, and rainfall records provide insight into the mechanism and activity patterns of an extremely slow urbanized landslide. Landslides 17:445–457. https://doi.org/10.1007/s10346-019-01276-7
Yunjun Z, Fattahi H, Amelung F (2019) Small baseline InSAR time series analysis: unwrapping error correction and noise reduction. Comput Geosci 133:104331. https://doi.org/10.1016/j.cageo.2019.104331

Supplementary Information The online version contains supplementary material available at https://doi.org/10.1007/s10346-024-02292-y.

Guadalupe Bru (✉) · Pablo Ezquerro · Rosa M. Mateos · Marta Béjar-Pizarro · Carolina Guardiola-Albert
Geohazards InSAR laboratory and modelling group (InSARlab), Geological Risk and Climate Change Department, Geological and Mining Institute of Spain (IGME-CSIC), Ríos Rosas 23, 28003 Madrid, Spain
Email: g.bru@csic.es

Jose M. Azañón
Department of Geodynamics, Faculty of Science, University of Granada, Av. de la Fuente Nueva, 18071 Granada, Spain

Meaza Tsige
Department of Geodynamics, Stratigraphy and Paleontology, Faculty of Geological Sciences, Complutense University, José Antonio Novais, 12, 28040 Madrid, Spain